Energy Efficiency Analysis and Optimization of Multiantenna Heterogeneous Cellular Networks Modeled by Matérn Hard-core Point Process

Yonghong Chen[1,2], Jie Yang[3*], Xuehong Cao[1,3] and Shibing Zhang[4]
[1]Department of Communication and Information Engineering, Nanjing University of Posts and Telecommunications, Nanjing, China
[e-mail: chenyh1107@ntu.edu.cn]
[2]Xinglin College, Nantong University, Nantong, China
[3]Department of Communication Engineering, Nanjing Institute of Technology, Nanjing, China
[e-mail: yangjie@njit.edu.cn]
[4]School of Electronics and Information, Nantong University, Nantong, China
*Corresponding author: Jie Yang

Abstract

The Poisson point process (PPP) is widely used in wireless network modeling and performance analysis because it can provide tractable results for heterogeneous cellular networks (HetNets) analysis. However, it cannot accurately reflect the spatial distribution characteristics of the actual base stations (BSs). Considering the fact that the distribution of macro base stations (MBSs) is exclusive, the deployment of MBSs is modeled by the Matérn hard-core point process (MHCPP), and the deployment of pico base stations (PBSs) is modeled by PPP. This paper studies the performance of multiantenna HetNets and improves the energy efficiency (EE) of HetNets by optimizing the transmit power of PBSs. We use a simple approximate method to study the signal-to-interference ratio (SIR) distribution in two-tier MHCPP-PPP HetNets and derive the coverage probability, average data rate and EE of HetNets. Then, an optimization algorithm is proposed to improve the EE of HetNets. Finally, three transmission technologies are simulated and analyzed. The results show that multiantenna transmission has better system performance than single antenna transmission and that selecting the appropriate transmit power for a PBS can effectively improve the EE of the system. In addition, two-tier MHCPP-PPP HetNets have higher EE than two-tier PPP-PPP HetNets.

Keywords: Energy efficiency, Multiantenna, Heterogeneous cellular networks, Matérn hard-core point process, Coverage probability

---

1. Introduction

$\mathbf{C}$urrently, with the exponential growth of mobile data traffic, cellular networks are facing huge challenges. As is known, the traditional cellular networks structure using macro cells cannot support future demands. Heterogeneous cellular networks (HetNets) with both small cells and macro cells have been widely recognized as a solution for the rapid growth of mobile data traffic [1-3]. Stochastic geometry provides an effective tool to evaluate the performance of HetNets [4]. In [5], a tractable model for downlink HetNets is developed. The model consists of k-tiers base stations (BSs), the BSs at each tier are randomly deployed, and each tier has a different transmit power, data support rate and base station density. In addition, the multiple input multiple output (MIMO) is also an effective way to address the network traffic demand in the future [6]. In previous research, [7-8] studied the average throughput and energy consumption in multiantenna single tier networks. Considering the interaction between the different tiers in HetNets, [9] and [10] analyzed the coverage probability of multiantenna HetNets. Moreover, [9] gave the ranking results for the coverage probability and single user rate under three transmission technologies, such as single-input single-output (SISO), space division multiple access (SDMA), and single-user beamforming (SUBF).

Due to the rapid growth of wireless network energy consumption, energy efficiency (EE) as an important performance indicator has caused widespread concern in academia and industry [11-12]. The BS density is an important technology for reducing HetNets energy consumption. In [13], the effect of the small cell BSs density on EE of cellular networks was studied by using stochastic geometry. In [14], the optimal BS density in single-tier and two-tier cellular networks was also studied. The research reported in [15] deduced the optimal small cell density while considering both coverage and data rate constraints. BS sleep scheduling scheme was also found to be an effective way to reduce the total energy consumption and improve the energy efficiency [16-17]. To characterize the potential benefits of BS sleep scheduling, [18] analyzed the performance of different sleep scheduling strategies. In addition, in [18-20], the authors provided the EE optimization algorithm from the aspects of BS association strategy [19], BS cooperation strategy [20], and coordinated multipoint transmission [21]. However, these energy efficiency researches studies on HetNets were conducted based on the Poisson point process (PPP) model.

Although PPP has been heavily used for modeling the spatial characteristics of wireless networks, considering the exclusion between macro base stations (MBSs), a non-Poisson point process can better reflect the spatial distribution characteristics of the actual base station compared with a PPP. The research in [22] models the cellular networks as Ginibre point processes (GPPs) and analyzes the mean interference and coverage probability. The study in [23] modeled the spatial distribution of transmitters as a Poisson hard-core process in wireless networks, and provided approximations of the coverage probability by employing the quasi-Monte Carlo method. The Matérn hard core point process (MHCPP) is an important type of exclusion point process, which has been used in wireless network modeling [24-27]. Although the MHCPP models the networks well, it is difficult to find the exact distribution of the signal-to-interference ratio (SIR), which is the crux to analyzing the coverage probability and achievable data rate of the networks [28-29]. Therefore, it is almost impossible to determine the impact of parameters such as BS density and BS transmit power on network performance.

Fortunately, [30-33] proposed that the SIR distribution of non-Poisson point process networks can be approximated precisely by the PPP network, that is, the threshold θ is scaled by the SIR gain factor G, which is called approximate SIR analysis based on the PPP (ASAPPP). A recent work [34] provided an accurate analysis of the SIR Meta distribution in general HetNets based on the ASAPPP. Therefore, we study the EE of the HetNets based on ASAPPP method, in which MBSs are modeled by non-Poisson point process distribution. The EE analysis and optimization of multiantenna HetNets based on MHCPP have not been studied. This paper investigates the EE of the multiantenna HetNets, in which the deployment of MBSs is modeled by MHCPP. First, the SIR distribution of MHCPP is approximated by the gain method based on the mean interference to signal ratio (MISR), i.e., the shift of the Poisson curve. Next, the concrete expressions of the coverage probability, average achievable rate and EE of multiantenna HetNets are obtained. Then, an optimization algorithm is proposed to improve the EE of multiantenna HetNets by controlling the transmit power of the pico base station (PBS). Finally, the performance of the system is simulated and analyzed through three transmission technologies, SISO, SDMA and SUBF.

The rest of this paper is arranged as follows: Section 2 describes the system model. Section 3 presents the coverage probability, the average achievable rate of the multiantenna HetNets and the expression of the system energy efficiency. In Section 4, the golden section method is proposed to optimize the energy efficiency. The simulation results are discussed in Section 5, and the conclusions are given in Section 6.

2. System Model

We consider two-tier HetNets that are composed of two types of nodes, MBSs and PBSs. The structure diagram is shown in **Fig. 1**.
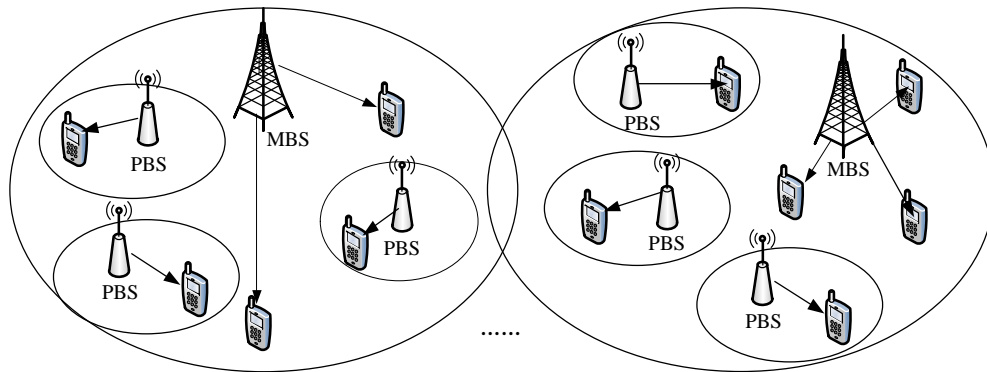

Fig. 1. Two-tier HetNets model

The MBSs are modeled by a MHCPP Φ_m with a density of λ_m, in which the distance between two nodes cannot be less than the given minimum distance. The MHCPP model aims to preserve the minimum distance r by deleting some nodes in a random point process. The generation process is as follows. First, a Poisson point process with intensity λ_b is generated as the parent process, and all of the points are marked independently, while the marked values are evenly distributed in the interval [0, 1]. Then all of the points are checked. Only when the marked value of a point is less than that of all points in the circle, whose center is the point and

that has a radius of *r*, the point will be retained; otherwise, the point will be deleted. After the deletion, the point process composed of the remaining points is called MHCPP, which can guarantee that the minimum distance between any two nodes is *r*. The PBSs and the users are deployed in the macro cell with the homogeneous Poisson point processes (HPPP) Φ_p and Φ_U, and their densities are λ_p and λ_u, respectively. Both the MBS and the PBS adopt the multiple antennas technology. The MBS is equipped with M_m transmit antennas, and the PBS is equipped with M_p transmit antennas. Their transmit power is μ_m and μ_p respectively. Using zero forcing precoding, each MBS serves N_m users in each resource block, and each PBS serves N_p users in each resource block. The transmit power of each BS will be distributed equally to its service users. All of the users have the same statistical characteristics, and each user has only one single receiving antenna.

    Due to the stability of the network model, only the typical user at the origin is considered. In addition, we consider the universal frequency reuse; in other words, all of the MBSs and PBSs share the same spectrum. The user will associate with the serving BS that receives the maximum average received signal power, and the received signal power for a typical user from the serving BS located at $x_0 \in \Phi_k$ is $\frac{\mu_k}{N_k} h_{k,x_0} \mid x_0 \mid^{-\alpha}$, with path loss exponent $\alpha > 2$, $k \in \{m, p\}$. We assume that the transmitter has perfect channel state information (CSI), and that the small scale fading on each link is Rayleigh fading. According to [9] and [10], the equivalent channel gain in the Rayleigh fading channel obeys the gamma distribution, i.e, the desired signal strength is $h_{k,x_0} \sim \Gamma(M_k + 1 - N_k, 1)$, and the interference signal strength is $h_{m,x_i} \sim \Gamma(N_m, 1)$, $h_{p,x_i} \sim \Gamma(N_p, 1)$. For simplicity, we use h_{k0}, h_{ki} instead of h_{k,x_0}, h_{k,x_i}. The cumulative interference power received by the typical user of HetNets from all other BSs is expressed as *I*. In the interference limited cellular network, the noise power can be ignored [5]. Therefore, the signal-to-interference ratio (SIR) of a typical user associated with the BS located at $x_0 \in \Phi_k$ can be expressed as

$$SIR_k = \frac{\frac{\mu_k}{N_k} h_{k,x_0} \mid x_0 \mid^{-\alpha}}{I} = \frac{\frac{\mu_k}{N_k} h_{k0} \mid x_0 \mid^{-\alpha}}{\sum_{x_i \in \Phi_m \setminus \{x_0\}} \frac{\mu_m}{N_m} h_{mi} \mid x_i \mid^{-\alpha} + \sum_{x_i \in \Phi_p \setminus \{x_0\}} \frac{\mu_p}{N_p} h_{pi} \mid x_i \mid^{-\alpha}} \ . \tag{1}$$

    Assuming that the user has open access, the user is allowed to access the BS at any tier. The probability of a typical user associated with a specific tier depends on the BS density and the transmit power of each tier. According to the Lemma 1 in [35], the probability of an association between a typical user and a macro tier is expressed by

$$A_m = \frac{\lambda_m \mu_m^{2/\alpha}}{\lambda_m \mu_m^{2/\alpha} + \lambda_p \mu_p^{2/\alpha}} \ . \tag{2}$$

and the probability of an association between a typical user and the PBS is expressed by

$$A_p = \frac{\lambda_p \mu_p^{2/\alpha}}{\lambda_m \mu_m^{2/\alpha} + \lambda_p \mu_p^{2/\alpha}} \ . \tag{3}$$

3. Energy Efficiency Analysis

3.1 Coverage Probability

In interference limited cellular networks, we define the coverage probability P_C as the probability that the *SIR* is larger or equal to a given threshold. Since the typical user is associated with at most one tier, the coverage probability can be expressed as the total probability of several disjoint events, i.e., $P_C = P_{C\_m} A_m + P_{C\_p} A_p$, where A_m and A_p represent the probability of a typical user associated with a macro tier and a pico tier, respectively, while P_{C_m} and P_{C_p} represent the coverage probability of the MBS and the PBS, respectively. P_{C_m} is defined as the probability that the serving MBS for a typical user provides a downlink SIR_m that is above a specific threshold θ_m, i.e., $P_{C\_m} = P(SIR_m > \theta_m)$ and P_{C_p} is defined as the probability that the serving PBS of a typical user provides a downlink SIR_p that is higher than a specific threshold θ_p, i.e., $P_{C\_p} = P(SIR_p > \theta_p)$.

It has been proved that the SIR distribution of non-Poisson point process networks can be approximated precisely by the PPP networks based on the ASAPPP, that is, the threshold θ is scaled by the SIR gain factor G, and the coverage probability of PPP networks is expressed as $P_c^{PPP}(\theta)$, i.e., $P_C(\theta) \approx P_c^{PPP}(\theta/G)$, which is called "approximate SIR analysis based on the PPP" (ASAPPP) [33],[36]. The defined asymptotic gain G can be expressed as $G = \dfrac{MISR_{PPP}}{MISR}$, where the MISR is the mean interference to average signal ratio. The study in [33] provides the conclusion that the MISR calculation result for the PPP networks is $MISR_{PPP} = 2/(\alpha - 2)$. The research in [37] provides the expression of the $MISR_{MHCPP}$ through simulation and data fitting as follows:

$$MISR_{MHCPP}(r, \alpha) = [a_1 + a_2 \cos(a_4 r) + a_3 \sin(a_4 r)]e^{-0.8996\alpha} + \frac{b_1 r^2 + b_2 r + b_3}{r^2 + b_4 r + b_5}, \tag{4}$$

where $a_1 = 15.22$, $a_2 = 3.684$, $a_3 = -2.033, $a_4 = 0.2536$, $b_1 = 0.261$, $b_2 = 0.1753$, $b_3 = 6.25$, $b_4 = 0.3243$, and $b_5 = 13.54$. Thus, the MISR-based gain of the MHCPP can be written as

$$G_m = \frac{MISR_{PPP}}{MISR_{MHCPP}} = \frac{2/(\alpha - 2)}{MISR_{MHCPP}}. \tag{5}$$

In a macro tier, the MBSs are modeled as a MHCPP. According to the MISR-based gain method, the coverage probability of the MBSs is derived. Assume that the given thresholds for the macro tier and the pico tier are equal, and the given threshold is θ. In the macro tier, the SIR_m of typical users can be written as

$$SIR_m = \frac{\dfrac{\mu_m}{N_m} h_{m0} |x_0|^{-\alpha}}{I} = \frac{\dfrac{\mu_m}{N_m} h_{m0} |x_0|^{-\alpha}}{\displaystyle\sum_{x_i \in \Phi_m \backslash \{x_0\}} \dfrac{\mu_m}{N_m} h_{mi} |x_i|^{-\alpha} + \sum_{x_i \in \Phi_p \backslash \{x_0\}} \dfrac{\mu_p}{N_p} h_{pi} |x_i|^{-\alpha}}$$

$$= \frac{h_{m0}}{\displaystyle\sum_{x_i \in \Phi_m \backslash \{x_0\}} h_{mi} |x_0|^{\alpha} |x_i|^{-\alpha} + \sum_{x_i \in \Phi_p \backslash \{x_0\}} \dfrac{\mu_p N_m}{\mu_m N_p} h_{pi} |x_0|^{\alpha} |x_i|^{-\alpha}} = \frac{h_{m0}}{I_1}. \tag{6}$$

The coverage probability of the MBSs modeled as a MHCPP is expressed as

$$P_{C\_m}(\theta) = P(SIR_m > \theta) = \int_{r_0>0} P(h_{m0} > \theta I_1 \mid r_0) f_m(r_0) dr_0$$

$$= \int_{r_0>0} E_{I_1}[e^{-\theta I_1} \sum_{i=0}^{M_m-N_m} \frac{(\theta I_1)^i}{i!}] f_m(r_0) dr_0 = \int_{r_0>0} \sum_{i=0}^{M_m-N_m} \frac{1}{i!} E_{I_1}[e^{-\theta I_1} \cdot (\theta I_1)^i] f_m(r_0) dr_0 \qquad (7)$$

$$= \int_{r_0>0} \sum_{i=0}^{M_m-N_m} \frac{1}{i!} (-\theta)^i \frac{\partial^i}{\partial(\theta)^i} L_{I_1}(\theta) f_m(r_0) dr_0 = \sum_{i=0}^{M_m-N_m} \frac{1}{i!} (-\theta)^i \frac{\partial^i}{\partial(\theta)^i} \int_{r_0>0} L_{I_1}(\theta) f_m(r_0) dr_0,$$

Where M_m is the transmit antennas number of MBS, N_m is the number of users served in each resource block by MBS, and $f_m(r_0)$ is the distance distribution between the service MBS and the macro user r_0 [35]

$$f_m(r_0) = 2\pi r_0 (\lambda_m + \lambda_p (\mu_p / \mu_m)^{2/\alpha}) \exp(-\lambda_m \pi r_0^2 - \lambda_p \pi (\mu_p / \mu_m)^{2/\alpha} r_0^2) , \qquad (8)$$

$$L_{I_1}(\theta) = E_{I_1}[e^{-\theta \cdot I_1}] = E_{I_1}[e^{-\theta(\sum_{x_i \in \Phi_m \backslash \{x_0\}} h_{mi} r_0^\alpha |x_i|^{-\alpha} + \sum_{x_i \in \Phi_p \backslash \{x_0\}} \frac{\mu_p N_m}{\mu_m N_p} h_{pi} r_0^\alpha |x_i|^{-\alpha})}]$$

$$\overset{(a)}{=} E_{\Phi_m, h_{mi}}[\prod_{x_i \in \Phi_m \backslash \{x_0\}} \exp(-\theta \cdot h_{mi} r_0^\alpha |x_i|^{-\alpha})] \cdot E_{\Phi_p, h_{pi}}[\prod_{x_i \in \Phi_p \backslash \{x_0\}} \exp(-\theta \frac{\mu_p N_m}{\mu_m N_p} h_{pi} r_0^\alpha |x_i|^{-\alpha})]$$

$$\overset{(b)}{\sim} E_{\Phi_m, h_{mi}}[\prod_{x_i \in \{\Phi_m \backslash \{x_0\}\}^{PPP}} \exp(-\frac{\theta}{G_m} h_{mi} r_0^\alpha |x_i|^{-\alpha})] \cdot E_{\Phi_p, h_{pi}}[\prod_{x_i \in \Phi_p \backslash \{x_0\}} \exp(-\theta \frac{\mu_p N_m}{\mu_m N_p} h_{pi} r_0^\alpha |x_i|^{-\alpha})]$$

$$\overset{(c)}{=} E_{\Phi_m}[\prod_{x_i \in \{\Phi_m \backslash \{x_0\}\}^{PPP}} L_{h_{mi}}(\frac{\theta}{G_m} r_0^\alpha |x_i|^{-\alpha})] \cdot E_{\Phi_P}[\prod_{x_i \in \Phi_p \backslash \{x_0\}} L_{h_{pi}}(\theta \frac{\mu_p N_m}{\mu_m N_p} r_0^\alpha |x_i|^{-\alpha})] \qquad (9)$$

$$\overset{(d)}{=} \exp(-2\pi \lambda_m \int_{r_0}^{\infty} (1 - L_{h_{mi}}(\frac{\theta}{G_m} r_0^\alpha |x|^{-\alpha})) x dx) \cdot \exp(-2\pi \lambda_p \int_{r_0}^{\infty} (1 - L_{h_{pi}}(\theta \frac{\mu_p N_m}{\mu_m N_p} r_0^\alpha |y|^{-\alpha})) y dy)$$

$$\overset{(e)}{=} \exp(-2\pi \lambda_m \int_{r_0}^{\infty} (1 - \frac{1}{(1 + \frac{\theta}{G_m} r_0^\alpha |x|^{-\alpha})^{N_m}}) x dx) \cdot \exp(-2\pi \lambda_p \int_{r_0}^{\infty} (1 - \frac{1}{(1 + \theta \frac{\mu_p N_m}{\mu_m N_p} r_0^\alpha |y|^{-\alpha})^{N_p}}) y dy)$$

$$\overset{(f)}{=} \exp(-\pi \lambda_m r_0^2 (\frac{\theta}{G_m})^{2/\alpha} \int_{(\frac{\theta}{G_m})^{-2/\alpha}}^{\infty} (1 - (\frac{1}{1 + u^{-\alpha/2}})^{N_m}) du) \cdot \exp(-\pi \lambda_p r_0^2 (\theta \frac{\mu_p N_m}{\mu_m N_p})^{2/\alpha} \int_{(\theta \frac{\mu_p N_m}{\mu_m N_p})^{-2/\alpha}}^{\infty} (1 - (\frac{1}{1 + v^{-\alpha/2}})^{N_p}) dv)$$

$$\overset{(g)}{=} \exp(-\pi \lambda_m r_0^2 (H(\frac{\theta}{G_m}, N_m) - 1)) \cdot \exp(-\pi \lambda_p r_0^2 (\frac{\mu_p}{\mu_m})^{2/\alpha} (H(\theta \frac{N_m}{N_p}, N_p) - 1)),$$

where (a) is defined according to the independence of the tiers, (b) uses the ASAPPP approximation method to move θ to $\frac{\theta}{G_m}$ and replace Φ_m with a PPP distribution, (c) is defined according to the channel powers independent of the BS positions, (d) is defined using the PPP probability generating functional (PGFL) [38], (e) is defined according to the Laplace transform of the $h_{mi} \sim \Gamma(N_m, 1)$ and $h_{pi} \sim \Gamma(N_p, 1)$, (f) denotes $(\frac{\theta}{G_m})^{-\frac{2}{\alpha}} x^2 r_0^{-2}$ by u and denotes $(\theta \frac{\mu_p N_m}{\mu_m N_p})^{-2/\alpha} y^2 r_0^{-2}$ by v, and (g) is ordered $H(x, y) = 1 + x^{2/\alpha} \int_{x^{-2/\alpha}}^{\infty} (1 - (1 + u^{-\alpha/2})^{-y}) du$.

From formulas (8) and (9), we can obtain

3372

Chen et al.: Energy Efficiency Analysis and Optimization of Multiantenna
Heterogeneous Cellular Networks Modeled by Matérn Hard-core Point Process

$$\int_{r_0>0} L_{I_1}(\theta)f_m(r_0)dr_0 = \frac{\lambda_m + \lambda_p(\dfrac{\mu_p}{\mu_m})^{2/\alpha}}{\lambda_m H(\dfrac{\theta}{G_m},N_m)+\lambda_p(\dfrac{\mu_p}{\mu_m})^{2/\alpha}H(\theta\dfrac{N_m}{N_p},N_p)} \ . \tag{10}$$

Therefore, the coverage probability of the MBS based on the MHCPP distribution can be expressed as follows:

$$P_{C\_m}(\theta) = \sum_{i=0}^{M_m-N_m} \frac{1}{i!}(-\theta)^i \frac{\partial^i}{\partial(\theta)^i}\left(\frac{\lambda_m + \lambda_p(\dfrac{\mu_p}{\mu_m})^{2/\alpha}}{\lambda_m H(\dfrac{\theta}{G_m},N_m)+\lambda_p(\dfrac{\mu_p}{\mu_m})^{2/\alpha}H(\theta\dfrac{N_m}{N_p},N_p)} \right). \tag{11}$$

Similarly, the coverage probability of the PBS can be calculated as

$$P_{C\_p}(\theta) = \sum_{i=0}^{M_p-N_p} \frac{1}{i!}(-\theta)^i \frac{\partial^i}{\partial(\theta)^i}\left(\frac{\lambda_p + \lambda_m(\dfrac{\mu_m}{\mu_p})^{2/\alpha}}{\lambda_p H(\theta,N_p)+\lambda_m(\dfrac{\mu_m}{\mu_p})^{2/\alpha}H(\theta\dfrac{N_p}{N_m},N_m)} \right). \tag{12}$$

Thus, the coverage probability of the two-tier HetNets can be written as

$$P_C = P_{C\_m}A_m + P_{C\_p}A_p$$

$$= \sum_{i=0}^{M_m-N_m} \frac{1}{i!}(-\theta)^i \frac{\partial^i}{\partial(\theta)^i}\left(\frac{1}{H(\dfrac{\theta}{G_m},N_m)+\dfrac{\lambda_p}{\lambda_m}(\dfrac{\mu_p}{\mu_m})^{2/\alpha}H(\theta\dfrac{N_m}{N_p},N_p)} \right) \tag{13}$$

$$+ \sum_{i=0}^{M_p-N_p} \frac{1}{i!}(-\theta)^i \frac{\partial^i}{\partial(\theta)^i}\left(\frac{1}{H(\theta,N_p)+\dfrac{\lambda_m}{\lambda_p}(\dfrac{\mu_m}{\mu_p})^{2/\alpha}H(\theta\dfrac{N_p}{N_m},N_m)} \right).$$

3.2 Average Achievable Rate

The average ergodic rate of a typical user associated with the macro tier and the pico tier is denoted by τ_m and τ_p. According to the definition of the average ergodic rate, τ_m and τ_p can be written as

$$\tau_m = \mathrm{E}(\log(1+SIR_m)] \tag{14}$$

and

$$\tau_p = \mathrm{E}(\log(1+SIR_p)] . \tag{15}$$

The locations of the MBSs Φ_m are modeled by MHCPP, and the average achievable rate is not easy to obtain directly. We first derived the expression for the average ergodic rate τ_m^{PPP} in the PPP networks, and then, according to the effective SIR gain method proposed in [39], by which the SIR distribution of the HetNets is approximated by moving the PPP curve with the SIR gain, and using the relationship between the coverage probability and achievable data rate obtained in [40], the average achievable rate τ_m^{MHCPP} of the MBSs modeled by the MHCPP distribution can be derived.

The expression for the average ergodic rate τ_m^{PPP} of the PPP networks can be expressed as follows:

$$\tau_m^{PPP} = E(\log(1+SIR_m)]$$

$$= \int_0^\infty f_m(r_0)E[\log(1+\frac{\frac{\mu_m}{N_m}h_{m0}r_0^{-\alpha}}{\sum_{x_i\in\Phi_m\backslash\{x_0\}}\frac{\mu_m}{N_m}h_{mi}x_i^{-\alpha} + \sum_{x_i\in\Phi_p\backslash\{x_0\}}\frac{\mu_p}{N_p}h_{pi}x_i^{-\alpha}})]dr_0, \tag{16}$$

where $f_m(r_0) = 2\pi r_0(\lambda_m + \lambda_p(\mu_p/\mu_m)^{2/\alpha})\exp(-\lambda_m\pi r_0^2 - \lambda_p\pi(\mu_p/\mu_m)^{2/\alpha}r_0^2)$ and

$$E[\log(1+\frac{\frac{\mu_m}{N_m}h_{m0}r_0^{-\alpha}}{\sum_{x_i\in\Phi_m\backslash\{x_0\}}\frac{\mu_m}{N_m}h_{mi}\mid x_i\mid^{-\alpha} + \sum_{x_i\in\Phi_p\backslash\{x_0\}}\frac{\mu_p}{N_p}h_{pi}\mid x_i\mid^{-\alpha}})]$$

$$= E_{\Phi_m,\Phi_p}[\log(1+\frac{\frac{\mu_m}{N_m}E[h_{m0}]r_0^{-\alpha}}{\sum_{x_i\in\Phi_m\backslash\{x_0\}}\frac{\mu_m}{N_m}E[h_{mi}]\mid x_i\mid^{-\alpha} + \sum_{x_i\in\Phi_p\backslash\{x_0\}}\frac{\mu_p}{N_p}E[h_{pi}]\mid x_i\mid^{-\alpha}})]$$

$$= E_{\Phi_m,\Phi_p}[\log(1+\frac{\frac{\mu_m}{N_m}(M_m+1-N_m)r_0^{-\alpha}}{\sum_{x_i\in\Phi_m\backslash\{x_0\}}\mu_m\mid x_i\mid^{-\alpha} + \sum_{x_i\in\Phi_p\backslash\{x_0\}}\mu_p\mid x_i\mid^{-\alpha}})] \tag{17}$$

$$= E_{\Phi_m,\Phi_p}[\log(1+\frac{\frac{M_m+1-N_m}{N_m}}{\sum_{x_i\in\Phi_m\backslash\{x_0\}}r_0^\alpha\mid x_i\mid^{-\alpha} + \sum_{x_i\in\Phi_p\backslash\{x_0\}}\frac{\mu_p}{\mu_m}r_0^\alpha\mid x_i\mid^{-\alpha}})]$$

$$= E_{\Phi_m,\Phi_p}[\log(1+\frac{\frac{M_m+1-N_m}{N_m}}{I_m})].$$

Following lemma 1 in [41], formula (17) can be written as

$$E_{\Phi_m,\Phi_p}[\log(1+\frac{\frac{M_m+1-N_m}{N_m}}{I_m})]$$

$$= \int_0^\infty \frac{1}{z}e^{-z}[E[e^{-z(I_m-1)}] - E[e^{-z(I_m-1+\frac{M_m+1-N_m}{N_m})}]]dz \tag{18}$$

$$= \int_0^\infty \frac{1-e^{-z\frac{M_m+1-N_m}{N_m}}}{z}E[e^{-zI_m}]dz.$$

The expression of $E[e^{-zI_m}]$ can be derived as follows:

$$E[e^{-zI_m}] = E[e^{-z\sum_{x_i\in\Phi_m\backslash\{x_0\}} r_0^\alpha|x_i|^{-\alpha} + \sum_{x_i\in\Phi_p\backslash\{x_0\}} \frac{\mu_p}{\mu_m} r_0^\alpha|x_i|^{-\alpha}}]$$

$$= E[\prod_{x_i\in\Phi_m\backslash\{x_0\}} e^{-zr_0^\alpha|x_i|^{-\alpha}}]\cdot E[\prod_{x_i\in\Phi_p\backslash\{x_0\}} e^{-z\frac{\mu_p}{\mu_m} r_0^\alpha|x_i|^{-\alpha}}] \qquad (19)$$

$$= \exp(-2\pi\lambda_m\int_{r_0}^\infty(1-e^{-zx^{-\alpha}r_0^\alpha})xdx)\cdot\exp(-2\pi\lambda_p\int_{r_0}^\infty(1-e^{-z\frac{\mu_p}{\mu_m}r_0^\alpha y^{-\alpha}})ydy).$$

Let $u = z^{-\frac{2}{\alpha}}x^2r_0^{-2}$ and $v = (z\frac{\mu_p}{\mu_m})^{-\frac{2}{\alpha}}y^2r_0^{-2}$; then, the expression for $E[e^{-zI_m}]$ can be written as

$$E[e^{-zI_m}] = \exp(-\pi\lambda_m r_0^2 z^{\frac{2}{\alpha}}\int_{z^{-2/\alpha}}^\infty(1-e^{-u^{-\alpha/2}})du)\cdot\exp(-\pi\lambda_p r_0^2(z\frac{\mu_p}{\mu_m})^{\frac{2}{\alpha}}\int_{(z\frac{\mu_p}{\mu_m})^{-\frac{2}{\alpha}}}^\infty(1-e^{-v^{-\alpha/2}})dv)$$

$$(20)$$

$$= \exp(-\pi\lambda_m r_0^2(H(z)-1))\cdot\exp(-\pi\lambda_p r_0^2(\frac{\mu_p}{\mu_m})^{\frac{2}{\alpha}}(H(z)-1)),$$

where $H(z) = 1 + z^{\frac{2}{\alpha}}\int_{z^{-2/\alpha}}^\infty 1-e^{-v^{-\alpha/2}}dv$.

By substituting formulas (17-20) into formula (16), we obtain

$$\tau_m^{PPP} = \int_0^\infty \frac{1}{z}(1-e^{-z\frac{M_m+1-N_m}{N_m}})\frac{1}{H(z)}dz. \qquad (21)$$

According to formulas (16-18), τ_m^{PPP} can be written as

$$\tau_m^{PPP} = \int_0^\infty f_m(r_0)\int_0^\infty \frac{1-e^{-z\frac{M_m+1-N_m}{N_m}}}{z}E[e^{-zI_m}]dzdr_0 = \int_0^\infty f_m(r_0)\int_0^\infty \frac{1-e^{-z\frac{M_m+1-N_m}{N_m}}}{z}L_{I_m^{PPP}}(z)dzdr_0. \qquad (22)$$

The coverage probability of the MBSs modeled as a PPP can be expressed as

$$P_c^{PPP}(z) = P(SIR_m^{PPP} > z) = P(h_{m0} > zI_m^{PPP})$$

$$= E_{I_m^{PPP}}[e^{-zI_1^{PPP}}\sum_{i=0}^{M_m-N_m}\frac{(zI_m^{PPP})^i}{i!}] = \sum_{i=0}^{M_m-N_m}\frac{1}{i!}(-z)^i\frac{\partial^i}{\partial(z)^i}L_{I_m^{PPP}}(z). \qquad (23)$$

According to [40] , $\tau_m^{PPP} = \int_0^\infty \frac{P_c^{PPP}(z)}{1+z}dz. \qquad (24)$

By substituting formula (23) into (24) and from formula (22) and (24), we can obtain the following expression:

$$\int_0^\infty \frac{\sum_{i=0}^{M_m-N_m}\frac{1}{i!}(-z)^i\frac{\partial^i}{\partial(z)^i}L_{I_m^{PPP}}(z)}{1+z}dz = \int_0^\infty f_m(r_0)\int_0^\infty \frac{1-e^{-z\frac{M_m+1-N_m}{N_m}}}{z}L_{I_m^{PPP}}(z)dzdr_0. \qquad (25)$$

According to the effective SIR gain method proposed in [39], we derive the following:

$$P_{C\_m}^{MHCPP}(z) = P_{C\_m}^{PPP}(z/\hat{G}_m) = P(h_{m0} > zI_m^{PPP}/\hat{G}_m) = \sum_{i=0}^{M_m-N_m}\frac{1}{i!}(-z)^i\frac{\partial^i}{\partial(z)^i}L_{I_m^{PPP}/\hat{G}_m}(z), \qquad (26)$$

where $\hat{G}_m = \frac{1}{1+\omega}(G_m-1)+1$, $\omega = \frac{\lambda_p}{\lambda_m}\left(\frac{\mu_p}{\mu_m}\right)^\delta$ and $\delta = 2/\alpha$.

According to formula (23) and (24), τ_m^{MHCPP} can be written as

$$\tau_m^{MHCPP} = \int_0^\infty \frac{P_c^{MHCPP}(z)}{1+z}dz = \int_0^\infty \frac{\sum_{i=0}^{M_m-N_m} \frac{1}{i!}(-z)^i \frac{\partial^i}{\partial(z)^i} L_{I_m^{PPP}/\hat{G}_m}(z)}{1+z}dz . \tag{27}$$

Comparing formula (25) and (27), we obtain the expression of τ_m^{MHCPP} as follows:

$$\tau_m^{MHCPP} = \int_0^\infty f_m(r_0)\int_0^\infty \frac{1-e^{-z\frac{M_m+1-N_m}{N_m}}}{z}L_{I_m^{PPP}/\hat{G}_m}(z)dzdr_0 = \int_0^\infty \frac{1}{z}(1-e^{-z\frac{M_m+1-N_m}{N_m}})\frac{1}{H\left(z/\hat{G}_m\right)}dz . \tag{28}$$

Similarly, the expression of τ_p can be obtained as follows:

$$\tau_p = \int_0^\infty \frac{1}{z}(1-e^{-z\frac{M_p+1-N_p}{N_p}})\frac{1}{H(z)}dz . \tag{29}$$

3.3 Power Consumption

The actual total power consumption of BS includes the circuit power consumption, signal processing power consumption, cooling power consumption, etc., which mainly depend on the total transmission power consumption and the number of active antennas at the transmitter [42-43]. The power consumption of each MBS and PBS is given by

$$P_m = \xi_m\mu_m + M_m P_{dynm} + P_{m0} \tag{30}$$

and

$$P_p = \xi_p\mu_p + M_p P_{dynp} + P_{p0} , \tag{31}$$

where μ_m and μ_p are the transmit power of the MBS and the PBS, and ξ_m and ξ_p are the load-dependent power consumption coefficients of the MBS and the PBS, respectively, which represent the power consumption variation with the traffic load of the MBS and PBS. M_m and M_p represent the number of antennas equipped by the MBS and the PBS, respectively. P_{dynm} and P_{dynp} represent the circuit power of their active transmit RF links. P_{m0} and P_{p0} represent the static power consumption of the MBS and the PBS, respectively. Since ξ_m and ξ_p are proportional to the traffic load of the MBS and PBS, we replace them with K_m and K_p, which are the number of users served by MBS and PBS, respectively. According to [35], K_m and K_p can be expressed as

$$K_m = \frac{A_m\lambda_u}{\lambda_m} , \tag{32}$$

and

$$K_p = \frac{A_p\lambda_u}{\lambda_p} . \tag{33}$$

Then, the power consumption of each MBS and PBS can be expressed as

$$P_m = K_m\mu_m + M_m P_{dynm} + P_{m0} , \tag{34}$$

and

$$P_p = K_p\mu_p + M_p P_{dynp} + P_{p0} . \tag{35}$$

Thus, the total power consumption of multiantenna HetNets can be written as

$$P_{total} = \lambda_m P_m + \lambda_p P_p . \tag{36}$$

3.4 Energy Efficiency

In this paper, we define EE as the ratio of the area average achievable rate to the total power consumption of the multiantenna HetNets as follows:

$$\eta_{EE} = \frac{\tau}{P_{total}} = \frac{\tau}{\lambda_m P_m + \lambda_p P_p} \ , \tag{37}$$

where τ is the area average achievable rate of the multiantenna HetNets. According to [9], τ can be defined as

$$\tau = \lambda_m N_m P_{C\_m} A_m \tau_m^{MHCPP} + \lambda_p N_p P_{C\_p} A_p \tau_p . \tag{38}$$

4. Energy Efficiency Optimization

Considering that the MBS is mainly used for basic coverage, its transmit power depends on the size of the coverage area. In this paper, we optimize the transmit power of the PBS to maximize the EE of multiantenna HetNets. Assuming that $\lambda_m, \lambda_p, \mu_m, M_m, M_p$ are fixed values, through numerical simulation, it is found that formula (37) is a unimodal function, which has a global best advantage. To facilitate the use of the convex optimization algorithm to solve the problem, formula (37) should be reversed. The optimization problem can be expressed as follows:

$$\min_{\mu_p} -\eta_{EE}$$
$$s.t. \ \mu_p < \mu_m, \ \mu_p > 0. \tag{39}$$

Depending on the nature of the convex function, any extreme point of convex function on the convex set is also its optimal point. In this paper, the golden section method is used to get the optimal value of the objective function. The specific algorithm is described as follows:

① First, define $f(x) = -\eta_{EE}(x)$, where the optimization variable μ_p is represented by the variable x, given the interval $[a, b]$, where $a = \mu_m/1000$, $b = \mu_m - \mu_m/1000$, and the accuracy of the calculation is $\varepsilon = \lambda_m/1000$.

② Compute $x_1=a+0.382(b-a)$, $x_2=a+0.618(b-a)$.

③ If $f(x_1) > f(x_2)$, proceed to the next step; otherwise, proceed to step ⑤ directly.

④ If $x_2 - x_1 < \varepsilon$, stop the calculation and output $x^* = x_2$; otherwise, let $a = x_1$, $x_1 = x_2$, and $x_2 = a+0.618(b-a)$, and go to step ③.

⑤ If $x_2 - x_1 < \varepsilon$, stop the calculation and output $x^* = x_1$; otherwise, let $b = x_2$, $x_2 = x_1$, and $x_1 = a+0.382(b-a)$, and go to step ③.

The optimal value μ_p^* can be obtained through the calculation of the above steps. Substituting μ_p^* into formula (37), we can obtain the maximum energy efficiency.

5. Simulation Results and Analysis

In this section, we use MATLAB software platform to provide the simulation results for the energy efficiency of multiantenna HetNets. Using the default simulation parameters for the system model shown in **Table 1**. In this section, the following three transmission technologies are simulated and compared between two-tier PPP-PPP HetNets and two-tier MHCPP-PPP HetNets.

(i) single-input single-output (SISO), that is, each BS serves only one user in each resource block;

(ii) single-user beamforming (SUBF), that is, the BS at the k-th tier with M_k antennas serves a single user, i.e., $N_k = 1$;

(iii) space division multiple access (SDMA), where the BS at the k-th tier with M_k antennas serves N_k users in each resource block. Here, we consider full SDMA, i.e., $M_k = N_k$.

Table 1. System parameters

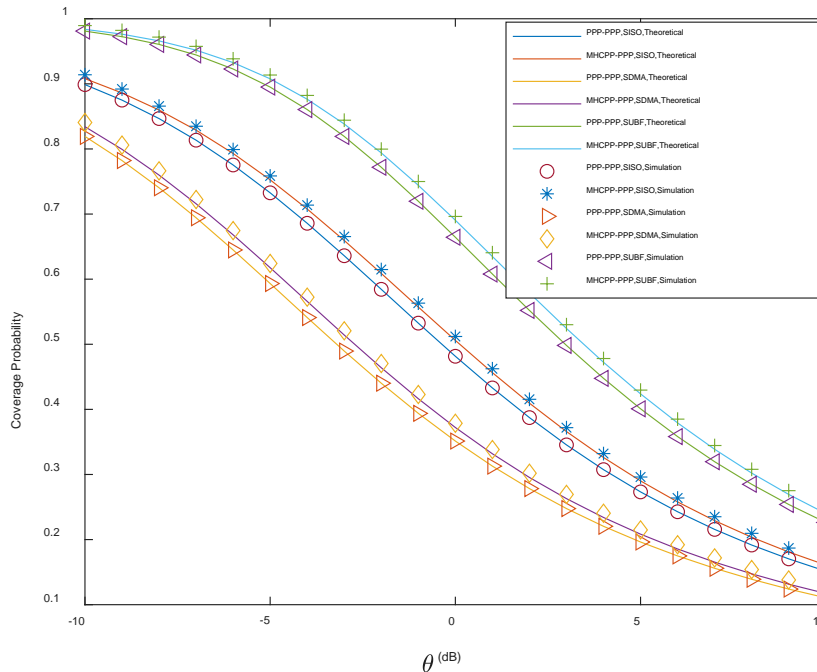| Parameters	Values
λ_m	10^{-3} m^{-2}
λ_u	0.1 m^{-2}
α	4
θ	0 dB
μ_m	40 W
M_m	2
M_p	2
r	10
P_{dynm}	16.9 W
P_{dynp}	6.8 W
P_{m0}	1000 W
P_{p0}	50 W

Fig. 2. Coverage probability versus SIR θ

Fig. 2 shows the comparison of the theoretical results and simulation results of the coverage probability for the two-tier MHCPP-PPP and two-tier PPP-PPP networks with different target

SIR θ values when $\lambda_p = 3\lambda_m$ and the three transmission technologies are used. It can be seen from **Fig. 2** that there is a very small gap between the simulation results and the corresponding theoretical results for the coverage probability of the two-tier MHCPP-PPP HetNets. This gap can be attributed to the interference approximation from the MHCPP tier to the PPP tier. Obviously, the approximate value of the coverage probability is excellent for a large range of θ values, which verifies the effectiveness of the ASAPPP-based method. It can also be seen from **Fig. 2** that when using the SUBF transmission technology, the system has the best coverage probability, followed by SISO and SDMA. The performance of the SUBF is better than that of the SISO, because the transmission performance of the service BS is improved by beamforming gain, and the fading power of its interference links is the same as that of SISO. The performance of SDMA is worse than that of SISO, due to the average fading power of their serving links is the same, while that of the interference links of SDMA increases.

The performances of the two-tier PPP-PPP HetNets and two-tier MHCPP-PPP HetNets are compared by using three transmission technologies. **Fig. 3** gives the relationship between the area average achievable rate and the transmit power of the PBSs, and **Fig. 4** gives the relationship between the EE and the PBS transmit power. From **Fig. 3** and **Fig. 4**, it can be seen that the SUBF provides a higher average achievable rate and EE than both SISO and SDMA due to the extra beamforming gain. The SDMA performs better than the SISO because the SDMA serves more users and provides a higher achievable rate. It can also be seen from **Fig. 4** that regardless of which transmission technology is used, the EE of the MHCPP-PPP HetNets is higher than that of the two-tier PPP-PPP HetNets, and the EE increases first and then decreases. There exists an optimal transmit power to achieve the optimum EE value. With the increase in the transmit power of the PBSs, a greater number of users will access the PBSs, the power of the PBS is smaller, thus the EE of the HetNets will be increased at this time. When the number of users with access reaches saturation, the increase of the PBS transmit power will increase the total power consumption and reduce the energy efficiency.
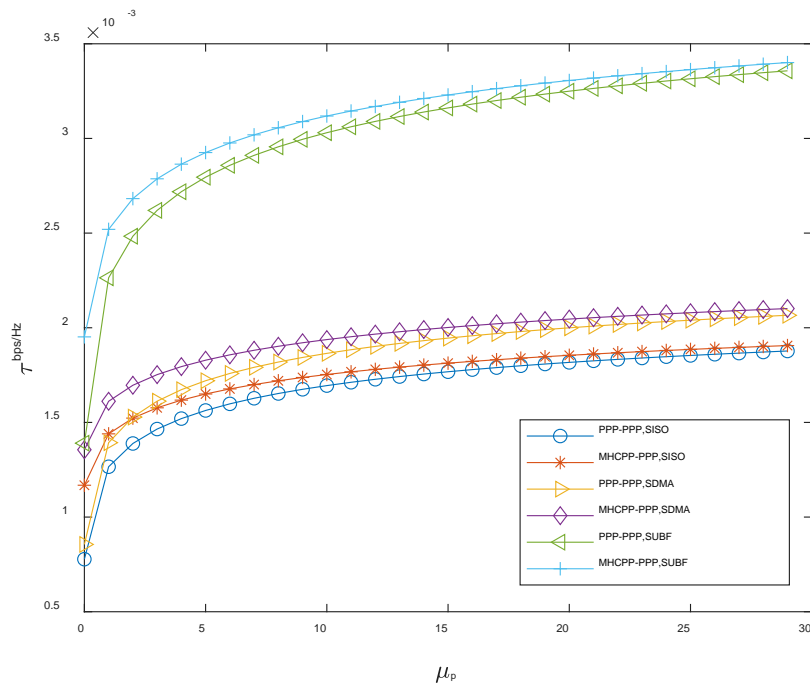

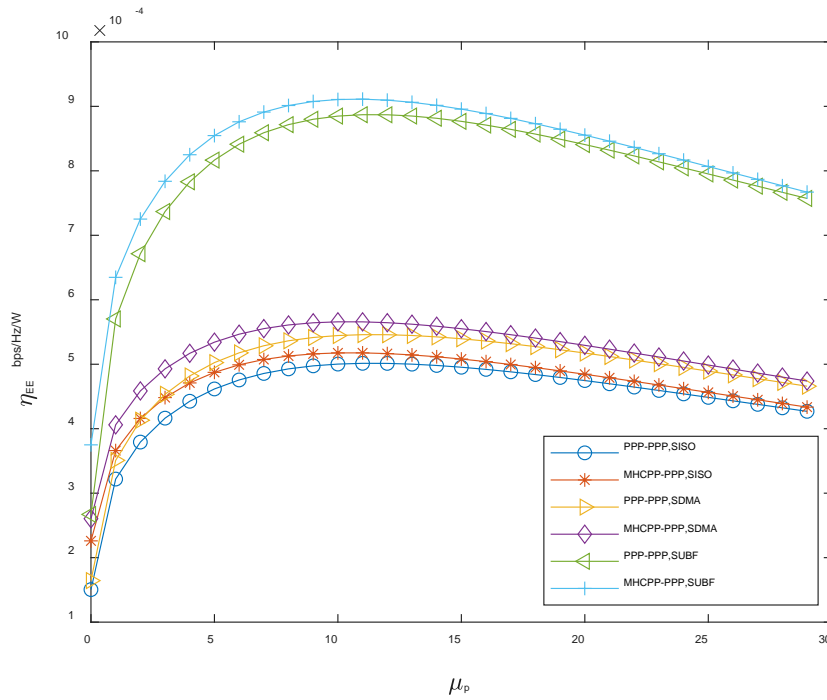**Fig. 3.** Average achievable rate versus the PBSs transmit power μ_p

Fig. 4. Energy efficiency η_{EE} versus the PBSs transmit power μ_p
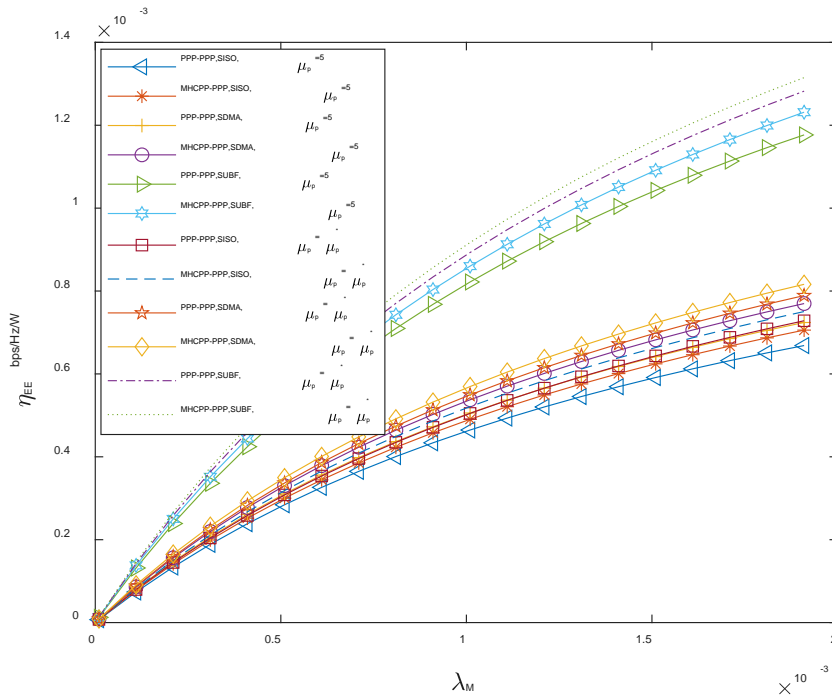

Fig. 5. Energy efficiency η_{EE} versus the MBSs densities λ_m

Fig. 5 describes the relationship between the EE of the two-tier HetNets and the density of the MBSs λ_m when $\lambda_p = 3\lambda_m$, and it gives the EE curves of the two-tier PPP-PPP HetNets and two-tier MHCPP-PPP HetNets when the system uses three transmission technologies in two cases. In one case, the transmit power of the PBS takes a fixed value of 5 W, and in the other case, the transmit power of the PBS takes the optimal value. The optimal value of PBS is obtained by the golden section method, and the simulation results when $\lambda_m = 10^{-3} m^{-2}$ are analyzed. In two-tier PPP-PPP HetNets, for SISO, SDMA, and SUBF, when the transmit power of the PBS takes the optimal value, the EE of HetNets is 8.6%, 8.7% and 8.7% higher than when the transmit power of the PBS takes the fixed value of 5 W, respectively. In addition, in two-tier MHCPP-PPP HetNets, for SISO, SDMA, and SUBF, when the transmit power of PBS takes the optimal value, the EE of HetNets is 6.2%, 5.9% and 6.6% higher than when the transmit power of the PBS takes the fixed value of 5 W, respectively. Therefore, setting the appropriate transmit power for PBS can effectively improve the EE of the HetNets. It can also be seen from **Fig. 5** that multiantenna transmission has better system performance than single-antenna transmission, especially when using SUBF transmission technology.

5. Conclusion

In this paper, we study the performance of multiantenna HetNets, in which the MBS is modeled by the MHCPP, and it improves the EE of HetNets by optimizing the transmit power of PBS. First, based on the simple approximation method of the SIR distribution, the coverage probability and average data rate are derived. Then, the EE of the two-tier multiantenna HetNets is deduced. Next, we use the golden section method to get the optimal PBS transmit power and to maximize the EE of the multiantenna HetNets. Finally, three transmission technologies, i.e., SISO, SDMA and SUBF are simulated and analyzed. The simulation results show that multiantenna transmission has better system performance than single antenna transmission, especially using SUBF transmission technology. In addition, regardless of which transmission technology is used, two-tier MHCPP-PPP HetNets is superior to PPP-PPP HetNets in terms of both the coverage probability and energy efficiency.

The results of this paper have certain reference value for the analysis of random space networks with multiantenna transmission, and they can provide some theoretical guidance for the practical operation of the PBSs. Future research directions will consider the joint optimization of parameters such as the minimum distance of two MBSs, the density of the PBSs and the transmit power of the PBSs.

References

[1] A. Ghosh, N. Mangalvedhe, R. Ratasuk, et al., "Heterogeneous cellular networks: From theory to practice," *IEEE Communications Magazine*, vol. 50, no. 6, pp. 54-64, 2012. Article (CrossRef Link)

[2] T. Yang, F. Heliot, and C. H. Foh, "A survey of green scheduling schemes for homogeneous and heterogeneous cellular networks," *IEEE Communications Magazine*, vol. 53, no. 11, pp. 175-181, Nov. 2015. Article (CrossRef Link)

[3] M. Peng, D. Liang, Y. Wei, J. Li, and H.-H. Chen, "Self-configuration and self-optimization in LTE-advanced heterogeneous networks," *IEEE Communications Magazine*, vol. 51, no. 5, pp. 36-45, May 2013. Article (CrossRef Link)

[4]   J. G. Andrews, F. Baccelli, and R. K. Ganti, "A tractable approach to coverage and rate in cellular networks," *IEEE Transactions on Communications*, vol. 59, no. 11, pp. 3122-3134, Nov. 2011. Article (CrossRef Link)

[5]   H. S. Dhillon, R. K. Ganti, F. Baccelli, et al., "Modeling and Analysis of K-Tier Downlink Heterogeneous Cellular Networks," *IEEE Journal on Selected Areas in Communications*, vol. 30, no. 3, pp.550-560, 2012. Article (CrossRef Link)

[6]   J. G. Andrews et al., "What will 5G be," *IEEE Journal on Selected Areas in Communications*, vol. 32, no. 6, pp. 1065-1082, Jun. 2014. Article (CrossRef Link)

[7]   R. Wang, J. Zhang, S. H. Song, and K. B. Letaief, "Average throughput analysis of downlink cellular networks with multi-antenna base stations," in *Proc. of IEEE International Symposium on Personal, Indoor, and Mobile Radio Communication (PIMRC)*, pp. 1892-1896, Sep. 2014. Article (CrossRef Link)

[8]   Z. Chen, L. Qiu, and X. Liang, "Area spectral efficiency analysis and energy consumption minimization in multi-antenna Poisson distributed networks," *IEEE Transactions on Wireless Communications*, vol. 15, no. 7, pp. 4862-4874, Jul. 2016. Article (CrossRef Link)

[9]   H. S. Dhillon, M. Kountouris, and J. G. Andrews, "Downlink MIMO HetNets: Modeling, ordering results and performance analysis," *IEEE Transactions on Wireless Communications*, vol. 12, no. 10, pp. 5208-5222, Oct. 2013. Article (CrossRef Link)

[10] C. Li, J. Zhang, J. G. Andrews, and K. B. Lataief, "Success probability and area spectral efficiency in multiuser MIMO HetHets," *IEEE Transactions on Communications*, vol. 64, no. 4, pp. 1544-1556, Apr. 2016. Article (CrossRef Link)

[11] X. Chen, J. Wu, Y. Cai, H. Zhang, and T. Chen, "Energy-efficiency oriented traffic offloading in wireless networks: A brief survey and a learning approach for heterogeneous cellular networks," *IEEE Journal on Selected Areas in Communications*, vol. 33, no. 4, pp. 627-640, Apr. 2015. Article (CrossRef Link)

[12] Q. Cui, T. Yuan, and W. Ni, "Energy-efficient two-way relaying under non-ideal power amplifiers," *IEEE Transactions on Vehicular Technology*, vol. 66, no. 2,pp. 1257-1270, Feb. 2017. Article (CrossRef Link)

[13] T. Zhang, J. Zhao, L. An, and D. Liu, "Energy efficiency of base station deployment in ultra dense HetNets: A stochastic geometry analysis," *IEEE Wireless Communications Letters*, vol. 5, no. 2, pp. 184-187, Apr. 2016. Article (CrossRef Link)

[14] L. Li, M. Peng, C. Yang, and Y. Wu, "Optimization of base-station density for high energy-efficient cellular networks with sleeping strategies," *IEEE Transactions on Wireless Communications*, vol. 65, no. 9, pp. 7501-7514, Sep. 2016. Article (CrossRef Link)

[15] Z. Wang and W. Zhang, "A separation architecture for achieving energyefficient cellular networking," *IEEE Transactions on Wireless Communications*, vol. 13, no. 6, pp. 3113-3123, Jun. 2014. Article (CrossRef Link)

[16] H. Chen, Q. Zhang and F. Zhao, "Energy-efficient base station sleep scheduling in relay-assisted cellular networks," *KSII Transations on Internet and Information Systems*, vol. 9, no. 3, pp. 1074-1086, May, 2015. Article (CrossRef Link)

[17] A. Dataesatu, P. Boonsrimuang, K. Mori, and P. Boonsrimuang, "Energy Efficiency Enhancement in 5G Heterogeneous Cellular Networks Using System Throughput Based Sleep Control Scheme," in *Proc. of International Conference on Advanced Communications Technology(ICACT)*, pp. 549-553, 2020. Article (CrossRef Link)

[18] Y. S. Soh, T. Q. S. Quek, M. Kountouris, and H. Shin, "Energy efficient heterogeneous cellular networks," *IEEE Journal on Selected Areas in Communications*, vol. 31, no. 5, pp. 840-850, May 2013. Article (CrossRef Link)

[19] C. H. Liu, K. L. Fong, "Fundamentals of the downlink green coverage and energy efficiency in heterogeneous networks," *IEEE Journal on Selected Areas in Communications*, vol. 34, no. 12, pp. 3271-3287, 2016. Article (CrossRef Link)

[20] C. Liu, B. Natarajan, H. Xia, "Small cell base station sleep strategies for energy efficiency," *IEEE Transactions on Vehicular Technology*, vol. 65, no. 3, pp. 1652-1661, 2016. Article (CrossRef Link)

[21] M. Xu, X. F. Tao, F. Yang, et al., "On energy efficient design for dynamic CoMP transmission in K-Tier heterogeneous cellular networks," *China Communications*, vol. 13, no. 6, pp. 147-153, 2016. Article (CrossRef Link)

[22] N. Deng, W. Zhou, M.Haenggi, "The Ginibre point process as a model for wireless networks with repulsion," *IEEE Transactions on Wireless Communications*, vol. 14, no. 1, pp. 107-121, 2015. Article (CrossRef Link)

[23] H. B. Kong, I. Flint, P. Wang, et al., "Modeling and analysis of wireless networks using poisson hard-core process," in *Proc. of IEEE International Conference on Communications*, May 21-25, 2017. Article (CrossRef Link)

[24] A. M. Ibrahim, T. ElBatt, and A. El-Keyi, "Coverage probability analysis for wireless networks using repulsive point processes," in *Proc. of IEEE 24th Annu. Int. Symp. Pers. Indoor Mobile Radio Commun. (PIMRC)*, pp. 1002-1007, September, 2013. Article (CrossRef Link)

[25] W. Bao and B. Liang, "Rate maximization through structured spectrum allocation and user association in heterogeneous cellular networks," *IEEE Transactions on Communications*, vol. 63, no. 11, pp. 4510-4524, Nov. 2015. Article (CrossRef Link)

[26] H. ElSawy and E. Hossain, "On cognitive small cells in two-tier heterogeneous networks," in *Proc. of 9th Int. Workshop Spatial Stochastic Models Wireless Netw. (SpaSWiN)*, pp. 75-82, May 2013. Article (CrossRef Link)

[27] H. He, P. Aquilina and T. Ratnarajah, "Full-duplex Multi-cell Networks with Interference Alignment," in *Proc. of 16th International Symposium on Wireless Communication Systems (ISWCS)*, August 27-30, 2019. Article (CrossRef Link)

[28] H. He, J. Xue, T. Ratnarajah, et al., "Modeling and analysis of cloud radio access networks using Matérn hard-core point processes," *IEEE Transactions on Wireless Communications*, vol. 15, no. 6, pp. 4074-4087, 2016. Article (CrossRef Link)

[29] H. ElSawy, E. Hossain, "Two-tier hetNets with cognitive femtocells: downlink performance modeling and analysis in a multichannel environment," *IEEE Transactions on Mobile Computing*, vol. 13, no. 3, pp. 649-663, 2014. Article (CrossRef Link)

[30] M. Haenggi, "The mean interference-to-signal ratio and its key role in cellular and amorphous networks," *IEEE Wireless Communications Letters*, vol. 3, no. 6, pp. 597-600, 2014. Article (CrossRef Link)

[31] R. K. Ganti, M. Haenggi, "SIR asymptotics in general cellular network models," in *Proc. of IEEE International Symposium on Information Theory (ISIT)*, pp. 1009-1013, June 14-19, 2015. Article (CrossRef Link)

[32] R. K. Ganti, M. Haenggi, "Asymptotics and approximation of the SIR distribution in general cellular networks," *IEEE Transactions on Wireless Communications*, vol. 15, no. 3, pp. 2130-2143, 2016. Article (CrossRef Link)

[33] M. Haenggi, "ASAPPP: A simple approximative analysis framework for heterogeneous cellular networks," in *Proc. of presented at Workshop Heterogeneous Small Cell Netw. (HetSNets'14)*, Dec. 2014. Article (CrossRef Link)

[34] S. S. Kalamkar, M. Haenggi, "Simple Approximations of the SIR Meta Distribution in General Cellular Networks," *IEEE Transactions on Communications*, vol. 67, no. 6, pp. 4393-4406, 2019. Article (CrossRef Link)

[35] H. S. Jo, Y. J. Sang, P. Xia, et al., "Heterogeneous cellular networks with flexible cell association: a comprehensive downlink SINR analysis," *IEEE Transactions on Wireless Communications*, vol. 11, no. 10, pp. 3484 - 3495, 2012. Article (CrossRef Link)

[36] H. C. Wei, N. Deng, W. Y. Zhou, et al., "A simple approximative approach to the SIR analysis in general heterogeneous cellular networks," in *Proc. of IEEE Global Communications Conference*, December 6-10, 2015. Article (CrossRef Link)

[37] J. Yang, Z. Y. Pan, J. C. Du, "Performance Analysis of Two-Tier Heterogeneous Cellular Networks Based on Poisson Hard-Core Process," in *Proc. of IEEE 19th International Conference on Communication Technology (IEEE ICCT2019)*, October 16-19, 2019.Article (CrossRef Link)

[38] D. Stoyan, W. S. Kendall, and J. Mecke, *Stochastic Geometry and Its Applications*, 2nd ed. John Wiley and Sons, 1995. Article (CrossRef Link)

[39] H. C. Wei, N. Deng, W. Y. Zhou, et al., "Approximate SIR analysis in general heterogeneous cellular networks," *IEEE Transactions on Communications*, vol. 64, no. 3, pp. 1259-1273, 2016. Article (CrossRef Link)

[40] G. Chen, L. Qiu, Z. Chen, "Area spectral efficiency analysis of multi-antenna networks modeled by Ginibre point process," *IEEE Wireless Communications Letters*, vol. 7, no. 1, pp. 6-9, February, 2018. Article (CrossRef Link)

[41] K. A. Hamdi, "A useful lemma for capacity analysis of fading interference channels," *IEEE Transactions on Communications*, vol. 58, no. 2, pp. 411-416, 2010. Article (CrossRef Link)

[42] D. Nguyen, L.-N. Tran, P. Pirinen, and M. Latva-aho, "Precoding for full duplex multiuser MIMO systems: spectral and energy efficiency maximization," *IEEE Transactions on Signal Processing*, vol. 61, no. 16, pp. 4038-4050, Aug. 2013. Article (CrossRef Link)

[43] J. Xu and L. Qiu, "Energy efficiency optimization for MIMO broadcast channels," *IEEE Transactions on Wireless Communications*, vol. 12, no. 2, pp. 690-701, Feb. 2013. Article (CrossRef Link)

YongHong Chen was born in Jiangsu Province, China, in 1981. She received the M.S. degree in signal and information processing from Nanjing University of Posts and Telecommunications in 2007. She is currently an Ph.D student at Nanjing University of Posts and Telecommunications, China. Now she is the vice professor of Xinglin College of Nantong University. Her research interests include heterogeneous and cellular networks, cooperative communications, and green communications.

Jie Yang was born in Jiangsu Province, China, in 1979. She received the B.S. and M.S. degrees from Lanzhou University of Technology in 2000 and 2003, respectively. She received PhD degree from Nanjing University of Post and Telecommunications in 2015. Now she is the vice professor of Nanjing Institute of Technology. Her currently research interests include cooperative communications, relaying network, and resource allocation.

Xuehong Cao was born in Suzhou, China, in 1964. She received the B.S. and M.S. degrees from the Nanjing University of Posts and Telecommunications in 1985 and 1988, respectively, and the Ph.D. degree in electronic engineering from Shanghai Jiaotong University in 1999. From 2004 to 2005, she worked as a visiting professor at the Department of Electrical Engineering, Stanford University. Now she is a Professor and the vice president of Nanjing Institute of Technology. Her research interests include multicarrier modulation, cooperative communication system and information theory.

Shibing Zhang is a professor of Nantong University from 2007. He received his Ph.D. degree from Nanjing University of Posts and Telecommunications, China in 2007. From Jul. 2009 to Mar. 2010, he was a visiting scholar of the Department of Electrical and Computer Engineering, University of Victoria, Canada. His research interests include wireless communications, OFDM system and cognitive radio.